

See discussions, stats, and author profiles for this publication at: <https://www.researchgate.net/publication/266743638>

Morphological, chemical and structural characterisation of deciduous enamel: SEM, EDS, XRD, FTIR and XPS analysis

Article in European Archives of Paediatric Dentistry. Official Journal of the European Academy of Paediatric Dentistry · September 2014

Source: PubMed

CITATIONS

14

6 authors, including:



Carmen Zamudio

Universidad Autónoma del Estado de México (UAEM)

2 PUBLICATIONS 26 CITATIONS

[SEE PROFILE](#)

READS

399



Rosalía Contreras-Bulnes

Universidad Autónoma del Estado de México (UAEM)

45 PUBLICATIONS 398 CITATIONS

[SEE PROFILE](#)



Rogelio J Scougall-Vilchis

Universidad Autónoma del Estado de México (UAEM)

102 PUBLICATIONS 817 CITATIONS

[SEE PROFILE](#)



Raul Alberto Morales Luckie

Universidad Autónoma del Estado de México (UAEM)

51 PUBLICATIONS 429 CITATIONS

[SEE PROFILE](#)

Some of the authors of this publication are also working on these related projects:



Project Synthesis and characterization of metal nanoparticles and nanocomposites [View project](#)



Project Molecule-based magnets made of coordination polymers [View project](#)



EUROPEAN JOURNAL OF PAEDIATRIC DENTISTRY

JOURNAL OF THE ITALIAN SOCIETY
OF PAEDIATRIC DENTISTRY (SIOI)

15

Volume 15 Number 3

3



In vitro analysis of extracted dens invaginatus using various radiographic imaging techniques
S. Rajasekharan, L. Martens, C. Vanhove, J. Aps

A
RIESDUE

EUROPEAN JOURNAL OF PAEDIATRIC DENTISTRY

Eur J Paediatr Dent
ISSN: 1591-996X
15 (3) 253-336 (2014)

EDITORIAL

Giuliano Falcolini
257

SCIENTIFIC PAPERS

258
C. Cardoso Silva, M. Maroto Edo, M. Soledad Álvaro Llorente,
E. Barbería Leache
Primary molar infraocclusion: frequency, magnitude, root
resorption and premolar agenesis in a Spanish sample

265
S. Rajasekharan, L. Martens, C. Vanhove, J. Aps
In vitro analysis of extracted *dens invaginatus* using various
radiographic imaging techniques

271
E. Ortu, F. Sgolastra, A. Barone, R. Gatto, G. Marzo,
A. Monaco
Salivary *Streptococcus Mutans* and *Lactobacillus* spp. levels
in patients during rapid palatal expansion

275
C. M. Zamudio-Ortega, R. Contreras-Bulnes,
R. J. Scougall-Vilchis, R. A. Morales-Luckie, O. F. Olea-Mejia,
L. E. Rodríguez-Vilchis
Morphological, chemical and structural characterisation of
deciduous enamel: SEM, EDS, XRD, FTIR and XPS analysis

281
M. Relvas, C. Coelho, C. Velazco Henriques, E. Ramos
Cariogenic bacteria and dental health status in adolescents:
the role of oral health behaviours

288
D. Angerame, M. De Biasi, L. Marigo, R. Castagnola, F. Somma,
A. Castaldo
Influence of simulated apical resorption following orthodontic
treatment on working length determination: an in vitro study

293
R. Rullo, F. Addabbo, F. Rullo, D. Di Maggio, V. M. Festa,
L. Brunet-Llobet, E. Lahor-Soler, J. Miranda-Rius
Oral pain due to severe pre-eruptive intracoronal resorption
in permanent tooth

L. Perillo
Speech outcome in unilateral complete cleft lip and palate
patients: a descriptive study

297
F. Guinot Jimeno, M. Mercadé Bellido, C. Cuadros Fernández,
A.I. Lorente Rodríguez, J. Llopis Pérez, JR. Boj Quesada
Effect of audiovisual distraction on children's behaviour,
anxiety and pain in the dental setting

303
G. D'Alessandro, I. Cremonesi, N. Alkhamis, G. Piana
Correlation between oral health in disabled children
and depressive symptoms in their mothers

309
A. Z. Zengin, P. Celenk, K. Gunduz, M. Canger
Primary double teeth and their effect on permanent successors

313
A. Baghalian, M. Ranjpur, T. Hooshmand, N. G. Herman,
A. Ebrahimi
Comparison of fracture resistance in post restorations
in primary maxillary incisors

317
F. Sengul, T. Gurbuz, S. Sengul
Finite element analysis of different restorative materials
in primary teeth restorations

323
M. D'Attilio, F. Festa, A. Filippakos, U. Comparelli, D. Tripodi
Third Class Resolver: a retrospective analysis

326
G.E. Salazar-Arboleda, A.M. Moncaleano-Arévalo,
A. M. Rueda-Chartouni, M. Barreto
Comparison of the upper airways from cephalometric
radiographs of children with and without finger-sucking habit

332
L. Brunet-Llobet, E. Lahor-Soler, J. Miranda-Rius
Oral pain due to severe pre-eruptive intracoronal resorption
in permanent tooth

C. M. Zamudio-Ortega*, R. Contreras-Bulnes*,
R. J. Scougall-Vilchis*, R. A. Morales-Luckie**,
O. F. Olea-Mejía**, L. E. Rodríguez-Vilchis*

Autonomous University of the State of Mexico, Toluca, México

*Center for Research and Advanced Studies in Dentistry (CIEAO),
Faculty of Dentistry

*Center for Research in Sustainable Chemistry
UAEM-UNAM (CCIQS). Faculty of Chemistry

e-mail: rcontrerasb@uaemex.mx

Morphological, chemical and structural characterisation of deciduous enamel: SEM, EDS, XRD, FTIR and XPS analysis

ABSTRACT

Aim The purpose of this study was to characterise the enamel surface of sound deciduous teeth in terms of morphology, chemical composition, structure and crystalline phases.

Materials and Methods The enamel of 30 human deciduous teeth was examined by: Scanning Electron Microscopy (SEM), Energy Dispersive X-Ray Spectroscopy (EDS), X-ray Powder Diffraction (XRD), Fourier Transform Infrared Spectroscopy (FTIR), and X-ray Photoelectron Spectroscopy (XPS). Chemical differences between incisors and canines were statistically evaluated using the Mann-Whitney U test ($p \leq 0.05$).

Results Three enamel patterns were observed by SEM: "mostly smooth with some grooves", "abundant microporosities" and "exposed prisms". The average Ca/P molar ratios were 1.37 and 1.03 by EDS and XPS, respectively. The crystallite size determined by XRD was $210.82 \pm 16.78 \text{ \AA}$. The mean ratio between Ca bonded to phosphate and Ca bonded to hydroxyl was approximately 10:1.

Conclusion The enamel of sound deciduous teeth showed two main patterns: "mostly smooth with some grooves" and "abundant microporosities". "Exposed prisms" was a secondary pattern. There were slight

variations among the Ca/P molar ratios found by EDS and XPS, suggesting differences in the mineral content from the enamel surface to the interior. The crystalline phases found in enamel were hydroxyapatite and carbonate apatite, with major type B than type A carbonate incorporation.

Keywords: Deciduous enamel, Energy dispersive X-ray spectroscopy, infrared spectroscopy, Scanning electron microscopy, X-ray diffraction, X-ray photoelectron spectroscopy.

Introduction

Nowadays the use of new technologies has deepened the knowledge on tooth structures. It has been reported that enamel is about 96 wt% (weight percentage) mineral, 3 wt% water and 1 wt% organic [Skinner, 2005]. The mineral component is an impure form of hydroxyapatite $[\text{Ca}_{10}(\text{PO}_4)_6(\text{OH})_2]$ because its lattice structure facilitates the incorporations of inorganic elements which are absent in the pure compound [Elliott et al., 2002; Eanes, 1979]. Additionally, as in other bioapatites, its Ca/P atomic ratio is lower than 1.67, the value for stoichiometric hydroxyapatite [Pasteris et al., 2008]. On the other hand, the organic phase has a protein nature [Simmer and Hu, 2001]. Specifically, deciduous enamel has unique characteristics related to the functions and permanency in mouth of the temporary dentition. It is worth mentioning that primary teeth have aprismatic enamel on their surface and percentages of Ca and P lower than permanent teeth [Ripa, 1966; De Menezes Oliveira et al., 2010]. However, most studies have been focused on permanent dentition or deciduous teeth with pathological processes [Mahoney et al., 2004; El-Sayed et al., 2010; Rizell et al., 2010; Keinan et al., 2006; Zilberman et al., 2010]. A deeper knowledge of the sound deciduous enamel would facilitate the adaptation of better prevention strategies and the synthesis of new biocompatible materials that promote the desired interactions with it. There have been some studies on this topic, but the information is still insufficient.

The purpose of this study was to characterise the enamel surface of sound deciduous teeth in terms of morphology, chemical composition, structure and crystalline phases.

Materials and methods

Deciduous teeth (incisors and canines), exfoliated or extracted because of their persistence in the mouth,

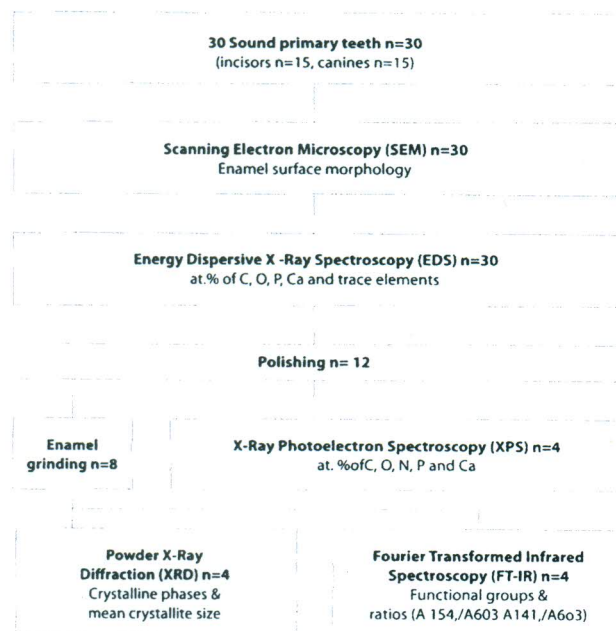


FIG. 1 Diagram of the procedures and characterisation techniques sequence.

were obtained under informed consent. The collected teeth did not present obvious decay or evidence of fluorosis, fractures or fillings. Immediately after extraction, they were placed in a plastic container with 0.2% thymol solution and transported to the laboratory within 15 days after extraction for analyses. Deionized water was used for the cleaning of the teeth; traces of soft tissue and blood were removed by means of a scalpel, specimens were delicately brushed with a soft brush (Sulcus, Oral-B, Mexico) and then finally rinsed with water. Storage was carried out in 0.2% thymol solution at 4 °C until the analyses were performed.

Each tooth was removed from the solution, rinsed with deionized water and dried with oil-free air from a triple syringe. The teeth were examined with a DIAGNOdent® pen (KaVo, Biberach, Germany), and 30 healthy teeth (15 incisors and 15 canines) with values between 0 and 13 were selected for characterisation. The sequence of the procedures and techniques applied is shown in figure 1.

Scanning Electron Microscopy (SEM)

Specimens were fixed to aluminium stubs with double-sided adhesive carbon tape (SPI Supplies, USA). Since we performed the analysis in the Low Vacuum Mode (25 Pa of chamber pressure), the application of a conducting coating was not necessary. Randomly selected buccal enamel surfaces were observed with a scanning electron microscope (JEOL, JSM-6510LV, Japan) at three different magnifications (200x, 600x and 1200x), with an electron acceleration voltage of 15–20 kV and using the backscattered electrons detector.

Energy Dispersive X-ray Spectroscopy (EDS)

The same buccal surface of each tooth was visualised under SEM at a standardised magnification of 100X with a working distance of 10 mm and the whole image area was selected to determine the atomic percentages (at%) of C, O, P, Ca and trace elements, using an X-ray detector system (Oxford Instruments, 7582, U.K.) attached to the scanning electron microscope.

Polishing

The enamel surface of each tooth was polished for 5 minutes with a rubber cup mounted at a low-speed handpiece of the dental unit (KaVo, Biberach, Germany) and under constant deionised water irrigation. Abrasive substances were not used.

Enamel grinding

The teeth were fractured hitting them with an agate mortar pestle, with the only purpose of leaving the dentin exposed. A micromotor with a round bur was used to remove the dentin and, when required, the teeth were fractured again to access areas that still contained dentin. Roots were cut when necessary using a carbide disc. Specimens were observed under stereoscopic microscope to ensure the complete removal of the dentin. The enamel pieces were washed by shaking them in deionised water to eliminate residual dentin powder, and then were air-dried. Finally, the pure enamel that remained was grinded in the agate mortar until a fine powder was obtained.

X-ray Powder Diffraction (XRD)

The powder of each specimen was placed in a circular glass specimen holder and was analysed in a powder X-ray diffractometer (D8 Advance, Bruker, Germany). We used the following conditions: CuK α X-ray radiation, X-ray source output power of 1050 W (35 kV, 30 mA), angular detector, 2 θ range of 7° to 67° with a step size of 0.02° and 0.5 seconds per step. A smooth factor of 0.1 was applied to improve the peak definition. The crystalline phases and structures, the spatial group and the crystallite size (using the Scherrer method) were determined with the EVA 13 program, belonging to the software suite DifracPlus Basic Evaluation Package (Bruker, Germany).

Fourier Transform Infrared Spectroscopy (FTIR)

Firstly, for each tooth analysed, 5 mg of enamel powder were mixed with 100 mg of KBr in an agate mortar and pellets transparent to visible light were fabricated on a manual hydraulic press with a pressure of 8.0 ton/cm². FTIR spectra were recorded with an Avatar 360 spectrometer (Thermo Nicolet, USA). The background noise was corrected with air data and iterations were performed for 32 times in the region of 200–4000 cm⁻¹ with a measurement resolution of 8 cm⁻¹. The spectral bands were analysed in the software OMNIC Macro

Basic v6.2 (Thermo Nicolet, USA) in order to assign the corresponding functional groups. The absorbance in the bands of carbonate (types A and B) and phosphate was measured from a previously traced baseline.

X-ray Photoelectron Spectroscopy (XPS)

The dental organs were first cut to obtain a 2.0 mm slice of each sample that was suitable for the XPS analysis. For this purpose, the pulp cavity was etched with orthophosphoric acid and filled with autopolymerizable resin (Unitek 3M, USA) for better support. Afterwards, the crown was fixed with a thermoplastic epoxy resin (Allied, USA) to a glass slide placed on a hot plate (Corning, USA). Each slide was then put on a cutter (South Bay Technology Inc., USA). The cut was done parallel to the buccal surface of the tooth (approx. 2 mm width) with a diamond wheel (South Bay Inc., USA) under constant water irrigation.

Subsequently, the samples were air-dried, fixed to aluminium stubs with carbon tape and were chemically analysed with an XPS (JEOL XPS-9200, Japan). The analysis area was 1 mm in diameter in the center of the buccal enamel surface. The chamber vacuum was at least 10^{-7} Pa. A Mg K α X-ray source was used at 200 W of power output. Peak positions were calibrated by referencing a value of 284.5 eV for the peak of C-C, C-H in the C 1s spectrum. Qualitative and semiquantitative data (at%) were obtained for C 1s, N 1s, O 1s, Ca 2p and P 2p from their respective high resolution spectra. The deconvolution of the XPS calcium spectrum was also done to determine the possible interactions of this element with other atoms in the enamel structure. The Handbook of X-ray Photoelectron Spectroscopy (JEOL, Japan) and the NIST XPS Database, Version 3.5 (NIST, USA) were used as reference of the characteristic binding energies (eV) related to each core atomic orbital of the studied elements.

Statistical analysis

Significant statistical differences in the atomic percentages of the elements and the Ca/P molar ratios between incisors and canines were analysed using the Mann-Whitney U test ($\alpha=0.05$), performed in the SPSS software, version 16.0 (SPSS Inc., Chicago, IL, USA).

Results

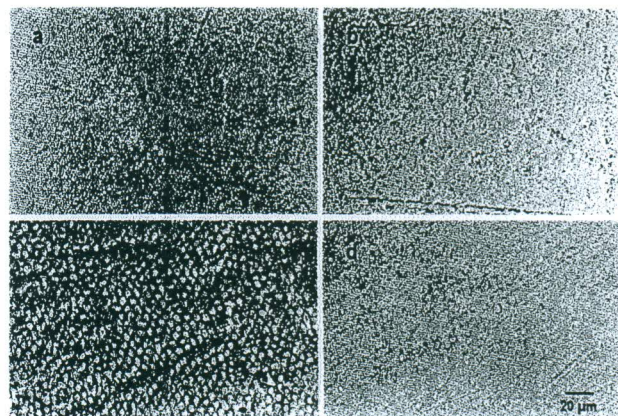


FIG. 2A-2D Enamel surface morphology patterns of deciduous teeth: a) mostly smooth with some grooves; b) abundant microporosities; c) exposed "key hole" prisms and d) exposed prisms in irregular circular-like shapes.

The enamel surface of deciduous teeth showed two main types of morphological patterns as observed by SEM:

A) "mostly smooth with some grooves" in 14 teeth (Fig. 2a);

B) "abundant microporosities" in 16 teeth (Fig. 2b).

"Exposed prisms" was a secondary pattern observed in the surface of 9 teeth, localised in all cases in the incisal third. Two teeth showed prisms with a "key hole" pattern (Fig. 2c), and seven teeth had prisms in irregular circular-like shapes (Fig. 2d).

The chemical composition of the enamel surface of the specimens obtained by EDS is shown in Table 1. The at% and Ca/P molar ratios (mean values and standard deviations) are presented. Incisors and canines showed no statistically significant differences in the at% of C, O, P, Ca and trace elements; nor the Ca/P molar ratios ($p \leq 0.05$).

The diffractograms of the incisors and canines analysed by XRD are shown in Fig. 3. The diffraction planes (labeled) corresponded, for all specimens, to the crystalline phases of hydroxyapatite and carbonate apatite. Both phases had hexagonal structure and belonged to the spatial group $P6_3/m$ (176), with the

	C	O	P	Ca	Trace elements*	Ca/P molar ratio
Incisors (n=15)	19.40±7.51	55.58±7.06	10.20±0.97	14.09±1.81	0.73±0.20	1.38±0.13
Canines (n=15)	15.18±6.06	58.77±6.44	10.72±1.06	14.68±2.12	0.65±0.13	1.36±0.08
P-value**	0.081	0.250	0.305	0.461	0.174	0.902
Total (n=30)	17.29±7.04	57.18±6.83	10.46±1.03	14.38±1.96	0.69±0.17	1.37±0.11

* at% lower than 1.0 (Cl + Na + Mg).

** Mann-Whitney U Test ($\alpha=0.05$)

TABLE 1 Mean values and standard deviations of elements atomic percentages and Ca/P molar ratios of deciduous enamel surface by EDS analysis.

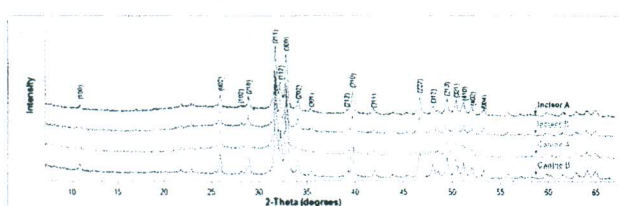


FIG. 3 X-ray diffractograms of the enamel powder of deciduous incisors and canines.

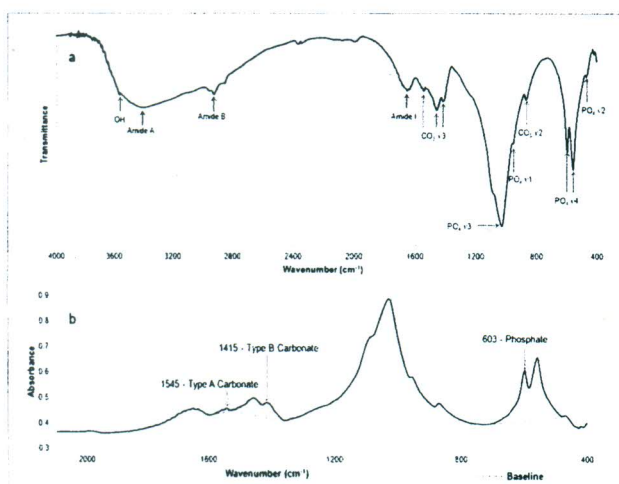


FIG. 4 Infrared spectra of deciduous incisor enamel: a) wide scan spectrum and b) narrow scan spectrum.

same unit cell dimensions ($a=b=9.44 \text{ \AA}$, $c=6.88 \text{ \AA}$). The mean crystallite size was $210.82 \pm 16.78 \text{ \AA}$.

The functional groups found in the enamel powder samples are shown in the wide scan FTIR spectrum (Fig. 4a). The typical OH stretching band was shown at 3566 cm^{-1} .

Regarding the phosphates, we could localize the $\text{PO}_4^{3-} \nu_1$ mode at 959 cm^{-1} , $\text{PO}_4^{3-} \nu_2$ mode at 472 cm^{-1} , $\text{PO}_4^{3-} \nu_3$ at 1033 cm^{-1} and $\text{PO}_4^{3-} \nu_4$ at 562 cm^{-1} with a less intense band centered at 603 cm^{-1} .

The major component of $\nu_2 \text{CO}_3^{2-}$, was type B carbonate (CO_3^{2-} ions substituting PO_4^{3-} sites), located at 872 cm^{-1} . Type B carbonate ν_3 mode presented two bands, one at 1415 cm^{-1} and the other at 1457 cm^{-1} . Type A carbonate (CO_3^{2-} substituting OH^- sites) in the ν_3 domain was located at 1545 cm^{-1} .

The amide I vibration arising from C=O stretching was centered in the 1654 cm^{-1} band. The amide A region, where the N-H stretching vibration of the amide appears, had its major intensity at 3396 cm^{-1} . The amide B region arising from C-H stretching, showed a band with higher intensity at 2927 cm^{-1} .

In addition, figure 4b shows the absorbance of the region where carbonates and phosphates appeared. The calculated mean ratios between carbonates and phosphates were: A_{1545}/A_{603} (type A carbonate/

C 1s	54.54
O 1s	24.66
P 2p3/2	8.28
Ca 2p3/2	8.79
N 1s	3.73
Ca/P molar ratio	1.03

TABLE 2 Mean values of elements atomic percentages and Ca/P molar ratios of deciduous enamel surface by XPS analysis.

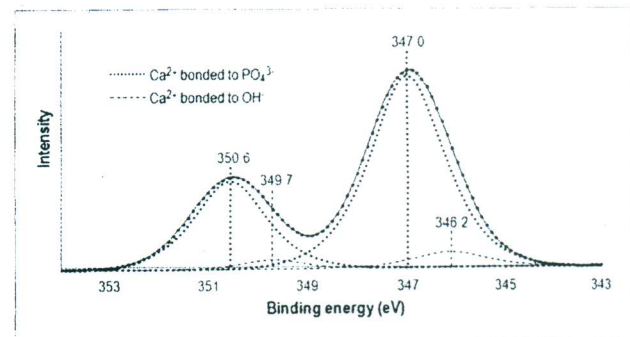


FIG. 5 Deconvolution of the XPS calcium spectrum from the enamel surface.

phosphate) = 0.0507 ± 0.009 and A_{1415}/A_{603} (type B carbonate/phosphate) = 0.2976 ± 0.031 .

The mean at% of C, O, P, Ca and N, as well as the average Ca/P molar ratio calculated from XPS spectra are shown in Table 2. The deconvolution of the XPS calcium spectrum (Fig. 5) show the binding energies (eV) in the peaks of Ca^{2+} bonded to PO_4^{3-} (higher peaks) and the peaks of Ca^{2+} bonded to OH^- (lower peaks). The average ratio between Ca bonded to phosphate and Ca bonded to hydroxyl was approximately 10:1.

Discussion

Since our goal was to study teeth without any physical or chemical modification after extraction from the oral cavity, the enamel surface was not polished nor etched before SEM analysis in order to maintain their original morphology and structure. The "mostly smooth with some grooves" pattern observed in this study could be explained by the fact that there is "prismless enamel" in the outermost layer of the deciduous teeth, where crystallites are regularly arranged parallel to each other [Kodaka et al., 1989]. The well-defined grooves found in some teeth might be formed due to the abrasion processes that all erupted teeth undergo [Fava et al., 1997], like the ones caused by toothbrushing or feeding. These findings are consistent with those of Neves et al. [2002], who obtained a similar SEM image of sound primary teeth without any treatment.

The "abundant microporosities" pattern was observed along the wear grooves, suggesting that these areas could be more prone to morphological and

structural changes resulting from factors inherent to the oral environment. Although microporosities could be more susceptible to bacteria adherence and more vulnerable to any carious process in comparison with smoother surfaces, it was not observed in our study.

Exposed prisms were found in the incisal third probably due to the presence of localized forces applied in this zone during the masticatory function. As reported by Kodaka et al. [1989], these areas showed "circular-like arcades" and arcade-shape prisms commonly named "key hole" prisms, where the head (rod) and tail (interrod) of each prism are clearly observed. However, contrary to our study, the teeth were etched with EDTA prior to SEM analysis.

Several authors [De Menezes Oliveira et al., 2010; Mahoney et al., 2004; Shore et al., 2010; Keinan et al., 2006; Zilberman et al., 2010] have used EDS to analyse the composition of human dental enamel. Nevertheless, there are variations in the results reported in the literature. Ca and P have been mainly evaluated, excluding other elements that form part of the hydroxyapatite structure, such as C and O [Mahoney et al., 2004; De Menezes Oliveira et al., 2010]. In our study, there was no difference between deciduous incisors and canines in terms of chemical content despite of the different formation, eruption and shedding times that could be influenced by several intrinsic and extrinsic factors. It is worth mentioning that the Ca/P molar ratio represents a relationship which is independent from the absence or presence of other elements, which constitutes a criterion to compare results, reason why it was used in our study. The calculated mean Ca/P molar ratio obtained was close although slightly lower than the 1.55-1.70 range reported by Shore et al. [2010] for deciduous enamel. On the other hand, it has been reported a Ca/P molar ratio around 1.74 for permanent teeth [Mahoney et al., 2004]. This suggests that there is a small difference between this molar ratio from deciduous and permanent teeth, though additional studies are required.

Another point to be highlighted is related to the indistinct use of the term phosphate (PO_4^{3-}) instead of phosphorus when referring to the element P, which leads to erroneous interpretations [Keinan et al., 2006; Zilberman et al., 2010]. Besides, results expressed in wt% as unit of measurement have been widely spread. Nonetheless, the at% is a more straightforward way to relate the number of atoms of each element, as used in this research.

With respect to the structural characterisation, there are important advantages when working with powdered enamel instead of fractured enamel for the XRD analysis. One is that all the plane directions are favoured for diffraction since all the grains are randomly oriented. A second advantage is that the geometry of the analysis is favoured when the powder inside the specimen holder is flattened, avoiding edge effects

such as secondary diffraction signals, etc. Therefore, these conditions promote more intense and defined diffraction peaks as well as less noise in the spectra for easier and more accurate analysis.

X-ray diffractograms showed narrow and well defined peaks, suggesting that the crystallite size was relatively large. Indeed, the calculated crystallite size coincided with the value reported by Leventouri et al. [2009] in deciduous teeth, which corresponds to a well crystallized apatite ($>200 \text{ \AA}$), according to Pleshko et al. [1991]. However, we could not determine by XRD analysis the proportion between hydroxyapatite and carbonate apatite, since their lattice parameters were the same and indistinguishable from each other.

FTIR, a useful tool for analysis of hydroxyapatite and the organic content in enamel, showed bands of the functional groups that coincided with other authors studies, such as: hydroxyl [Chang and Tanaka, 2002], phosphates [Chang and Tanaka, 2002; Sønju Clasen and Ruyter, 1997; Segvich et al., 2009; Markovic et al., 2004], carbonates [Chang and Tanaka, 2002; Leventouri et al., 2009; Rey et al., 1989; Sonju Clasen and Ruyter, 1997], and amides [Chang and Tanaka, 2002; Polyanichko and Wieser, 2007].

The carbonate/phosphate absorbance ratio as an indicator of the degree of incorporated carbonate in hydroxyapatite [Boskey and Mendelsohn, 2005], showed an increased presence of type B carbonate in relation to type A. Sønju Clasen and Ruyter [1997] reported that only about 11% of the total carbonate content in deciduous enamel is type A.

On the other hand, since XPS is a surface technique with an analysis scope of approximately 1 to 6 nm depth, we decided to polish the samples in order to eliminate the organic content over the enamel. It has been reported that the complete removal of the acquired pellicle is achieved pumicing the teeth around 5 minutes with a rotating rubber cup [Saxton, 1976], however, to prevent contamination, we did not use any abrasive. The presence of N and a high amount of C in the enamel surface may be due to two factors: one is that these elements are part of the proteins forming the organic pellicle that may not be completely eliminated and the second is that XPS is sensitive to environmental carbon. The at% of O, P and Ca were lower with XPS than when analyzed by EDS, probably due to the C at% increment. Additionally, the slight variations among the Ca/P molar ratios could be explained by the analysis depth of each employed technique, suggesting differences in the mineral content from the enamel surface to the interior.

An XPS advantage is that the chemical or electronic state of each element could be studied. As mentioned before, the average ratio between Ca^{2+} bonded to PO_4^{3-} and Ca^{2+} bonded to OH^- was approximately 10:1. In pure hydroxyapatite there are 9 Ca ions bonded to PO_4^{3-} for 1 Ca ion bonded to OH^- . The difference

can arise from CO_3^{2-} substitutions and other crystalline defects such as vacancies and interstitials; nevertheless, additional studies are required.

Conclusions

- Morphologically, the enamel of sound deciduous teeth showed two main patterns: "mostly smooth with some grooves" and "abundant microporosities". "Exposed prisms" was a secondary pattern located only in the incisal third.
- Chemically, there were slight variations among the Ca/P molar ratios found by EDS and XPS, suggesting differences in the mineral content from the enamel surface to the interior.
- Structurally, the crystalline phases found in enamel by powder XRD were hydroxyapatite and carbonate apatite; and there was a higher amount of incorporated type B carbonate than type A carbonate as evidenced by FTIR.

Acknowledgements

The authors deeply thank the personal and patients of the Pediatric Dental Clinics of the Autonomous University of the State of Mexico (UAEM) and of the Instituto de Salud del Estado de México (ISEM), for their support in the collection of the teeth. We highly acknowledge the contributions of Iván García, Claudia Centeno, Magdalena García and Gustavo López, for their helpful advice and suggestions.

References

- › Boskey AL, Mendelsohn R. Infrared spectroscopic characterization of mineralized tissues. *Vib Spectrosc* 2005;38:107-114.
- › Chang MC, Tanaka J. FT-IR study for hydroxyapatite/collagen nanocomposite cross-linked by glutaraldehyde. *Biomaterials* 2002;23:4811-8.
- › De Menezes Oliveira MA, Torres CP, Gomes-Silva JM, Chinelatti MA, De Menezes FC, Palma-Dibb RG, Borsatto MC. Microstructure and mineral composition of dental enamel of permanent and deciduous teeth. *Microsc Res Tech* 2010;73:572-7.
- › Eanes ED. Enamel Apatite: Chemistry, Structure and Properties. *J Dent Res* 1979;58:829-834.
- › El-Sayed W, Shore RC, Parry DA, Inglehearn CF, Mighell AJ. Ultrastructural analyses of deciduous teeth affected by hypocalcified amelogenesis imperfecta from a family with a novel Y458X FAM83H nonsense mutation. *Cells Tissues Organs* 2010;191:235-9.
- › Elliott JC, Wilson RM, Dowker SEP. Apatite structures. *Adv X Ray Anal* 2002;45:172-181.
- › Fava M, Watanabe I-S, Fava-de-Moraes F, Costa LRdRSd. Prismless enamel in human non-erupted deciduous molar teeth: a scanning electron microscopic study. *Revista de Odontologia da Universidade de São Paulo* 1997;11.
- › Keinan D, Smith P, Zilberman U. Microstructure and chemical composition of primary teeth in children with Down syndrome and cerebral palsy. *Arch Oral Biol* 2006;51:836-43.
- › Kodaka T, Nakajima F, Higashi S. Structure of the so-called 'prismless' enamel in human deciduous teeth. *Caries Res* 1989;23:290-6.
- › Leventouri T, Antonakos A, Kyriacou A, Venturelli R, Liarakopis E, Perdikatis V. Crystal structure studies of human dental apatite as a function of age. *Int J Biomater* 2009;2009:698547.
- › Mahoney EK, Rohanizadeh R, Ismail FS, Kilpatrick NM, Swain MV. Mechanical properties and microstructure of hypomineralised enamel of permanent teeth. *Biomaterials* 2004;25:5091-100.
- › Markovic M, Fowler BO, Tung MS. Preparation and comprehensive characterization of a calcium hydroxyapatite reference material. *J Res Natl Inst Stand Technol* 2004;109:553-568.
- › Neves AdeA, Castro RdeA, Coutinho ET, Primo LG. Microstructural analysis of demineralized primary enamel after in vitro toothbrushing. *Pesqui Odontol Bras* 2002;16:137-43.
- › Pasteris JD, Wopenka B, Valsami-Jones E. Bone and tooth mineralization: why apatite? *Elements* 2008;4:97-104.
- › Pleshko N, Boskey A, Mendelsohn R. Novel infrared spectroscopic method for the determination of crystallinity of hydroxyapatite minerals. *Biophys J* 1991;60:786-93.
- › Polyanichko AM, Wieser H. Vibrational circular dichroism and its applications to protein studies. In: Uversky VN, Permyakov EA, editors. *Methods in protein structure and stability analysis: vibrational spectroscopy*. New York: Nova Publishers; 2007. pp. 267-302.
- › Rey C, Collins B, Goehl T, Dickson IR, Glimcher MJ. The carbonate environment in bone mineral: a resolution-enhanced Fourier Transform Infrared Spectroscopy Study. *Calcif Tissue Int* 1989;45:157-64.
- › Ripa LW. The histology of the early carious lesion in primary teeth with special reference to a "prismless" outer layer of primary enamel. *J Dent Res* 1966;45:5-11.
- › Rizell S, Kjellberg H, Dietz W, Noren JG, Lundgren T. Altered inorganic composition of dental enamel and dentin in primary teeth from girls with Turner syndrome. *Eur J Oral Sci* 2010;118:183-90.
- › Saxton CA. The effects of dentifrices on the appearance of the tooth surface observed with the scanning electron microscope. *J Periodontal Res* 1976;11:74-85.
- › Segovich SJ, Smith HC, Kohn DH. The adsorption of preferential binding peptides to apatite-based materials. *Biomaterials* 2009;30:1287-98.
- › Shore RC, Backman B, Elcock C, Brook AH, Brookes SJ, Kirkham J. The structure and composition of deciduous enamel affected by local hypoplastic autosomal dominant amelogenesis imperfecta resulting from an ENAM mutation. *Cells Tissues Organs* 2010;191:301-6.
- › Simmer JP, Hu JC. Dental enamel formation and its impact on clinical dentistry. *J Dent Educ* 2001;65:896-905.
- › Skinner HCW. *Biominerals*. Mineral Mag 2005;69:621-641.
- › SØnju Clasen AB, Ruyter IE. Quantitative determination of type A and type B carbonate in human deciduous and permanent enamel by means of Fourier transform infrared spectrometry. *Adv Dent Res* 1997;11:523-7.
- › Zilberman U, Zilberman S, Keinan D, Elyahu M. Enamel development in primary molars from children with familial dysautonomia. *Arch Oral Biol* 2010;55:907-12.